

REVIEW

Open Access



Redox-controlled mechanisms of C and H isotope fractionation between silicate melt and COH fluid in the Earth's interior

Bjorn Mysen

Abstract

The behavior of COH fluids, their isotopes (hydrogen and carbon), and their interaction with magmatic liquids are at the core of understanding formation and evolution of the Earth. Experimental data are needed to aid our understanding of how COH volatiles affect rock-forming processes in the Earth's interior. Here, I present a review of experimental data on structure of fluids and melts and an assessment of how structural factors govern hydrogen and carbon isotope partitioning within and between melts and fluids as a function of redox conditions, temperature, and pressure.

The solubility of individual COH components in silicate melts can differ by several orders of magnitude and ranges from several hundred ppm to several wt%. Silicate solubility in fluid can reach several molecular at mantle temperatures and pressures. Different solubility of oxidized and reduced C-bearing species in melts reflects different solution equilibria. These equilibria are $2\text{CH}_4 + \text{Q}^n = 2\text{CH}_3^- + \text{H}_2\text{O} + \text{Q}^{n+1}$ and $2\text{CO}_3^{2-} + \text{H}_2\text{O} + 2\text{Q}^{n+1} = \text{HCO}_3^- + 2\text{Q}^n$, under reducing and oxidizing conditions, respectively. In the Q^n -notations, the superscript, n , denotes the number of bridging oxygen in the silicate species (Q-species).

The structural changes of carbon and silicate in magmatic systems (melts and fluids) with variable redox conditions result in hydrogen and carbon isotope fractionation factors between melt, fluid, and crystalline materials that depend on redox conditions and can differ significantly from 1 even at magmatic temperatures. The ΔH of D/H fractionation between aqueous fluid and magma in silicate–COH systems is between -5 and 25 kJ/mol depending on redox conditions. The ΔH values for $^{13}\text{C}/^{12}\text{C}$ fractionation factors are near -3.2 and 1 kJ/mol under oxidizing and reducing conditions, respectively. These differences are because energetics of O–D, O–H, O– ^{13}C , and O– ^{12}C bonding environments are governed by different solution mechanisms in melts and fluids.

From the above data, it is suggested that (COH)-saturated partial melts in the upper mantle can have δD values 100%, or more, lighter than coexisting silicate-saturated fluid. This effect is greater under oxidizing than under reducing conditions. Analogous relationships exist for $^{13}\text{C}/^{12}\text{C}$. At magmatic temperatures in the Earth's upper mantle, $^{13}\text{C}/^{12}\text{C}$ of melt in equilibrium with COH-bearing mantle in the -7 to -30% range increases with temperature from about 40 to $> 100\%$ and 80 – 120% under oxidizing and reducing conditions, respectively.

Keywords: Fluid, Solubility, Structure, Spectroscopy, Redox, Stable isotopes

Correspondence: bmysen@carnegiescience.edu
Geophysical Laboratory, Carnegie Instn. Washington, Washington DC, USA

Introduction

The budget, recycling, and evolution of COH volatiles are central to our understanding of many geochemical and geophysical properties of the interior of the Earth. The behavior of COH volatiles, therefore, is a very important factor in the processes that governed the formation and evolution of the solid Earth and perhaps other terrestrial planets (Ardia et al. 2013; Armstrong et al. 2015).

The speciation and activity/concentration of volatiles are particularly relevant to melting and crystallization. For carbon-bearing species, for example, reduced and oxidized C behaves quite differently (Saxena and Fei 1988; Ulmer and Luth 1991). These factors can govern melt composition (see also Kushiro 1974, 1998; Eggler 1975; Eggler and Baker 1982; Gaetani and Grove 1998; Foley et al. 2009). For example, the clearly different effects of CO₂ and CH₄ on melting and crystallization of model magma systems are evident in the example in Fig. 1. The response of the liquidus boundary between forsterite and enstatite in the NaAlSiO₄-Mg₂SiO₄-SiO₂-COH system to changing volatile species at high pressure illustrates such effects (Taylor and Green 1987). This boundary defines the activity of SiO₂ in the system and moves from SiO₂ deficient to SiO₂-enriched when carbon is reduced from CO₂ to CH₄ (Fig. 1). In fact, the effect of CH₄ is not that different from the effect of H₂O. This difference is also the underlying explanation for redox melting in the mantle (Song et al. 2009).

The stable isotope behavior is critical to monitor budgets and recycling of volatiles (Van Soest et al. 1998; Dixon et al. 2002; Kingsley et al. 2002; Javoy 2004). Volatile components in the COH system, when

dissolved in magmatic liquids, can affect stable isotope fractionation between the melt and coexisting fluids and crystalline materials (Dobson et al. 1989; Matthey et al. 1990; Deines 2002). Moreover, the redox state of the volatile components such as hydrogen, carbon, and perhaps sulfur can affect their influence on stable isotope fractionation in magmatic systems (Poulson 1996; Deines 2002).

In order to employ stable isotope behavior such as those of hydrogen and carbon to deduce processes of formation and evolution of the Earth's interior, experimental data are necessary. With such tools, we can address how, in particular, COH volatiles and their isotopes fractionate between magmatic liquids, fluids, and crystallizing materials as a function of redox conditions temperature and pressure. Data from samples analyzed after quenching to ambient conditions have been reported (Dobson et al. 1988; Matthey et al. 1990; Matthey 1991). However, extrapolation of such data to conditions during equilibration of magmatic liquids with fluids and crystals at high temperature and pressure is quite challenging because both fluids and melts commonly alter their structure, and sometimes their composition, during quenching to ambient temperature and pressure conditions (Kuroda et al. 1982; Baker and Stolper 1994; Zhang and Frantz 2000; Mysen and Yamashita 2010). That nature of those alterations can vary depending on the temperature–pressure quenching path. It is, therefore, better to determine the isotope fractionation while the samples are at the high temperature and pressure under controlled redox conditions relevant to magmatic processes in the Earth's interior. In this report, I will present

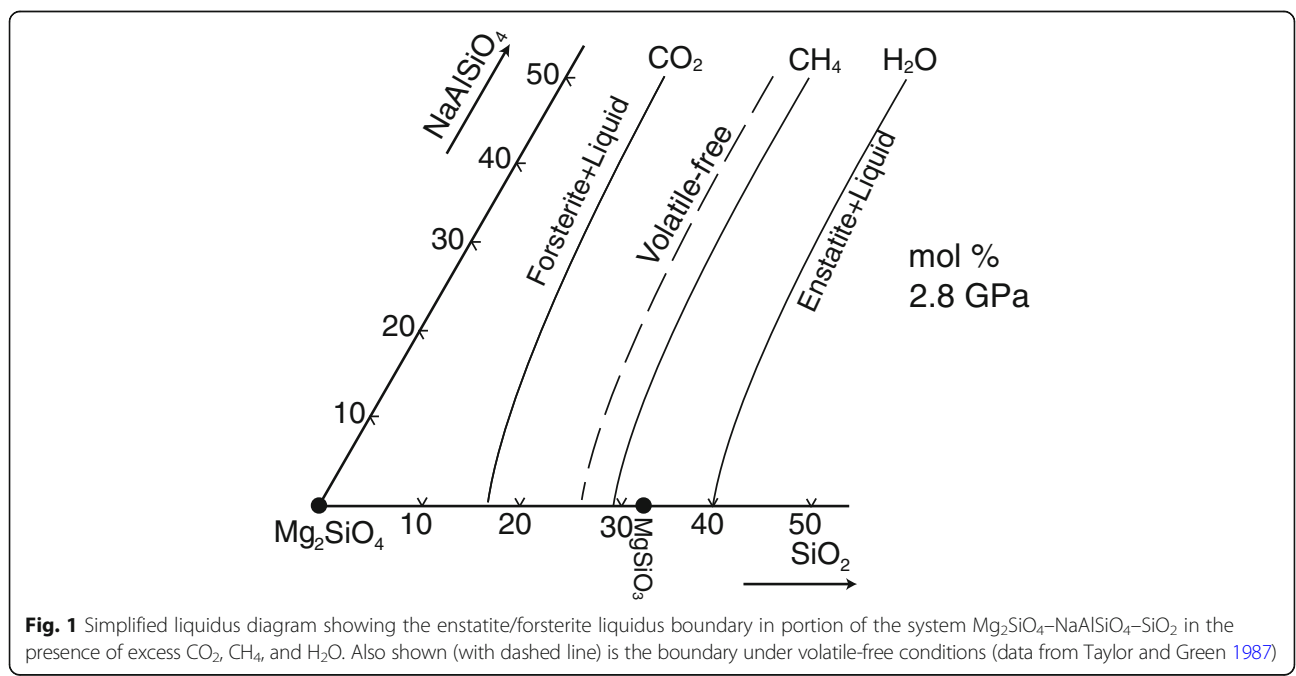


Fig. 1 Simplified liquidus diagram showing the enstatite/forsterite liquidus boundary in portion of the system Mg₂SiO₄-NaAlSiO₄-SiO₂ in the presence of excess CO₂, CH₄, and H₂O. Also shown (with dashed line) is the boundary under volatile-free conditions (data from Taylor and Green 1987)

and discuss recent experimental data relevant to these questions and illustrate with a few examples how the composition and redox state of COH volatiles affect carbon and hydrogen stable isotope fractionation between melts and fluids under conditions corresponding to those of the deep crust and upper mantle.

Review

A description and discussion of how carbon and hydrogen isotopes fractionate between fluids and melts at high temperature and pressure and with variable redox conditions is the focus of this presentation. Most of the experimental work on this subject have been carried out by using externally heated hydrothermal anvil cell method (Bassett et al. 1996) where the samples can be probed by vibrational spectroscopy while at the desired conditions. It should be noted that in these diamond cell experiments, temperature is an independent variable. Pressure is generated by the fluid in sample chambers of approximately constant volume and measured with probes such as the one-phonon shift of carbon-13 diamond embedded in the sample (Schiferl et al. 1997). It is for this reason that pressure is included as an upper horizontal axis in some of the figures in this presentation.

Vibrational spectroscopies, such as Raman and infrared not only can be used to probe structure but may also be employed to determine isotope ratios. Most of the experimental data discussed in this report were obtained by such methods. This technique can be used because the frequency ratio of vibrations of two oscillators that differ only in their mass (e.g., two isotopes) ν_1/ν_2 , is proportional to the square root of their mass ratio, $\sqrt{m_1/m_2}$. Provided that the cross section for a given vibration is not dependent on the type of isotope, 1 and 2, the ratio of integrated areas of the vibrational spectra, A_1/A_2 , equals their abundance ratio, X_1/X_2 . Data in support of this conclusion exist for the oxygen isotopes, ^{16}O and ^{18}O , (McKay et al. 2013) and hydrogen isotopes (Dalou et al. 2015).

With those caveats in mind, isotope ratios can be obtained by both transmission infrared absorption and by Raman spectroscopy. Moreover, the samples can be probed with those methods while at the desired conditions. Raman spectroscopy has an advantage over infrared spectroscopy in that Raman spectroscopic intensities do not depend on sample density, whereas infrared absorption intensity does. Densities of coexisting phases at high temperature and pressure often are not available. Laser beams used in microRaman measurements typically are 1–2 μm across and with confocal optics penetrate less than 30 μm into the sample (depending on optical transparency). Measurements with transmission microinfrared absorption have less spatial resolution with a minimum aperture of approximately $30 \times 30 \mu\text{m}$.

In addition, in infrared transmission spectroscopy, one has to ensure that only the sample of interest is in the optical path.

In addition to isotope ratios, it is also possible to ascertain the speciation and abundance ratio of the volatiles and the silicate components in silicate–COH systems from Raman and infrared spectroscopic data. Sometimes, it has also been possible to determine isotope fractionation between individual volatile species such as CO_3 and HCO_3 groups in silicate melts and coexisting, silicate-saturated melts, while these phases were at the temperature, pressure, and redox conditions of interest (Mysen 2015a, 2016, 2017). Further details of the experimental and analytical methods used for this purpose can be found in those papers and Dalou et al. (2015).

Although solubility of volatile components in silicate melts is not the focus of this report, solubility information is necessary in order to characterize the isotope behavior. Solubility of COH components can also be determined spectroscopically, using either infrared or Raman spectroscopy (Scholze 1960; Behrens et al. 2004, 2006). Traditionally, analyses have been conducted on quenched materials, but recent technical advances now allow infrared and Raman spectroscopy to be used to determine the concentration of at least some volatiles while the samples are at the desired temperatures and pressures (Behrens and Yamashita 2008; Le Losq et al. 2015).

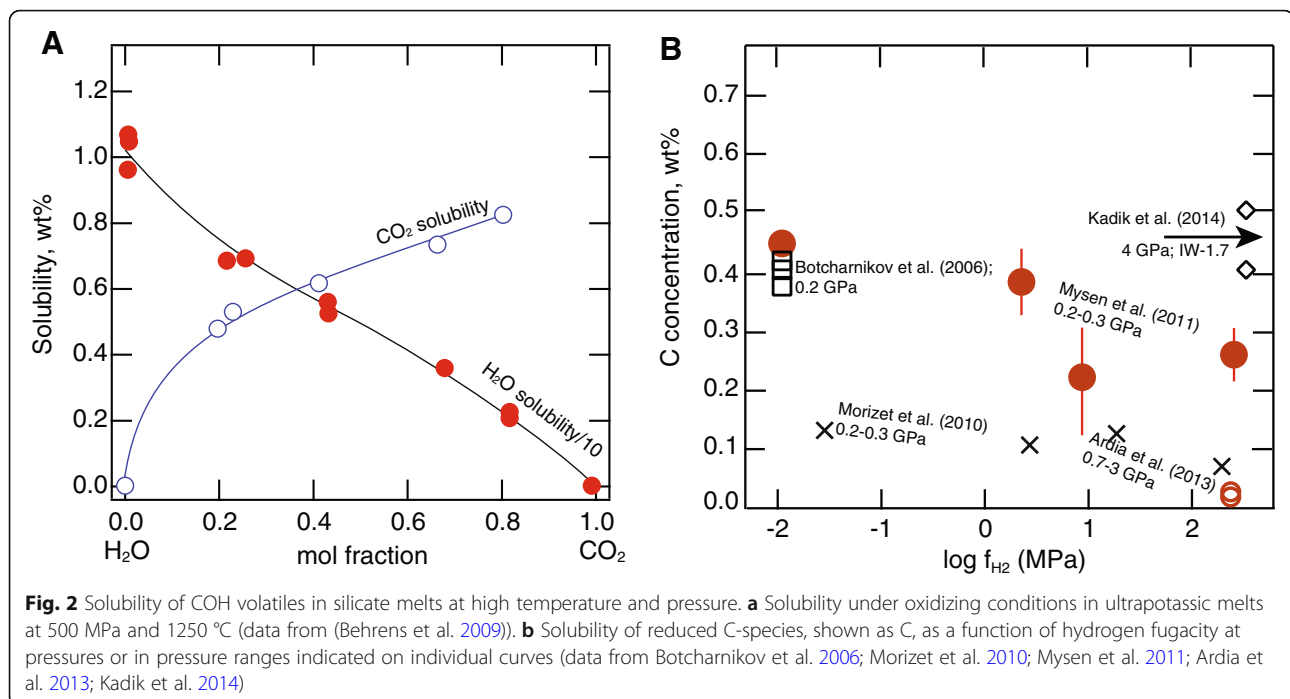
Solubility and solution mechanisms

Fractionation of stable isotopes between coexisting melts and fluids can be linked to solubility and solution mechanisms of volatiles in melts and of silicate in coexisting COH fluids. The principles that govern solubility in coexisting melts and fluids have been reviewed extensively elsewhere (Paillat et al. 1992; Newton and Manning 2008) and will not be discussed further here.

COH volatiles in melts

Determination of the solubility of H_2O and CO_2 in silicate–COH melts requires sufficiently oxidizing conditions so that carbon-bearing species more reduced than that of carbon in CO_2 are unimportant. Those conditions correspond to oxygen fugacities at or above that somewhere between that defined by the NNO (nickel–nickel oxide) and QFM (quartz–magnetite–fayalite) buffer (Mysen et al. 2011). In other words, CO_2 – H_2O mixtures will be the principal species in environments such as those of subduction zone melting, for example (Wood et al. 1990; Arculus 1994).

The solubilities of neither H_2O nor CO_2 are simple linear functions of the $\text{CO}_2/\text{H}_2\text{O}$ abundance ratio of the system (Fig. 2a; see also Behrens et al. 2009). This



non-linear solubility behavior is at least in part because of non-ideal mixing behavior of CO_2 – H_2O fluids (Eggler et al. 1979; Aranovich and Newton 1999). In addition, silicate melt– CO_2 – H_2O mixtures also are non-ideal (Papale et al. 2006) which adds to the non-linear behavior of CO_2 and H_2O solubility in Fig. 2a.

Reduced carbon species may be encountered in the deep Earth where redox conditions approach those described by the IW (iron-wüstite) buffer and below (Frost and McCammon 2008; Rohrbach et al. 2011). Even lower oxygen fugacity appears to have existed during the early core-forming stages of the Earth (O'Neill 1991; Righter and Drake 1999). Under such conditions, the dominant C-bearing species in the COH system likely is methane, CH_4 . Molecular H_2 can also play a significant role and contribute more than 10% of the volatile species under such very reducing conditions (Kadik et al. 2014). Its solubility in silicate at high temperature and pressure is greater than that which would be expected if hydrogen simply existed as molecular H_2 . There is some evidence to suggest that H_2 interacts chemically with the silicate melt to form OH-groups (Luth and Boettcher 1986; Luth et al. 1987).

More experimental solubility data exist for carbon in melts as a function of redox conditions (Morizet et al. 2010; Mysen et al. 2011; Ardia et al. 2013). Some of the data are summarized for various melt and magma compositions in Fig. 2b. It is evident that as carbon undergoes reduction, its solubility in silicate melt decreases. However, there is considerable variation in available solubility data so that, for example, even the solubility of CH_4 in basalt composition melt at several GPa pressure

and upper mantle temperatures has been reported between about a hundred ppm C (Fig. 2b; see also Ardia et al. 2013; Armstrong et al. 2015) to several thousand ppm (Kadik et al. 2004, 2014). The reasons for this wide solubility range are not clear, but may be related to experimental difficulties controlling the speciation of COH volatiles under extremely reducing conditions.

Silicate solubility in fluid

Less is known about silicate solubility in COH composition fluids than about solubility of COH volatiles in silicate melts at high temperatures and pressures. Quantitative experimental data have been reported for silicates and aluminosilicates in pure H_2O (Manning et al. 2010; Hunt et al. 2011; Manning and Aranovich 2014). The silicate solubility can reach several molecular (Newton and Manning 2008). There is, in fact, a second critical endpoint in the SiO_2 – H_2 system between 0.9 and 1 GPa (Kennedy et al. 1962). Solubility of silica and other oxide components also depends on the presence of other components such as, in particular alkalis and alumina, which when occurring together, can cause major solubility enhancements because of formation of multicomponent complexes in the fluid (Pascal and Anderson 1989; Mysen and Armstrong 2002; Manning 2004; Mysen 2012).

Solution mechanisms

Water in melts and fluids

It has been known for some time that solution of water in silicate melts is in the form of molecular H_2O and as

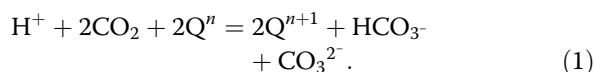
OH-groups that form bonding to cations such as Si^{4+} , Al^{3+} , alkalis, and alkaline earths (Stolper 1982; Cody et al. 2005; Xue and Kanzaki 2008). The extent to which network-modifying cations such as alkalis and alkaline earths form bonds with OH-groups in aluminosilicate– H_2O systems appears somewhat sensitive to the electronic properties of the cations as well as their proportion relative to network-forming Si^{4+} and Al^{3+} (Xue and Kanzaki 2008). Little is known about this latter feature in aluminosilicate–COH systems.

In silicate– H_2O systems, water in aqueous fluids at high temperature and pressure does dissolve silicate components (Manning 2004) in which at least some of the oxygen in silicate tetrahedra are replaced by OH-groups (Zotov and Keppler 2002; Mibe and Bassett 2008; Mysen 2009). Such structural features recently also have been observed in Raman and infrared spectra of silicate-saturated COH fluid (Mysen, unpublished data). However, whether in silicate– H_2O or silicate–COH systems at high temperature and pressure, the abundance ratio, OH/ H_2O , in melts always is greater than that in fluid (Mysen 2010). This difference is greater in silicate–COH fluids than in silicate– H_2O fluids.

Carbon species

Under oxidizing conditions, carbon-bearing species in melts and fluids at high temperature and pressure are dominated by CO_2 , CO_3 , and HCO_3 . In hydrous C-bearing systems such as silicate–COH, the dominant species are of HCO_3 and CO_3 type with limited evidence for molecular CO_2 . The limited existence of CO_2 is in part because it has been found that molecular CO_2 becomes decreasingly important with increasing H_2O content of silicate melts (King and Holloway 2002). The latter conclusion is also consistent with the general observation that abundance of molecular CO_2 species diminishes as a silicate melt becomes depolymerized, which does, indeed happen with solution of H_2O (Cody et al. 2005). It follows, therefore, that CO_2 might be an unimportant species in silicate–COH melt, which is consistent with the lack of observed signals from molecular CO_2 in such melts (Mysen 2015a, 2015b).

The relationship between carbonate stability (CO_3^{2-} and HCO_3^-) and molecular CO_2 in silicate melts and perhaps silicate-rich COH fluids in principle can be written as:

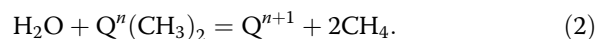


In Eq. (1) the Q^n and Q^{n+1} formalism expresses silicate species with in this case n and $n+1$ bridging oxygen, respectively. Recent NMR-based evidence

suggest that the carbonate groups form isolated clusters (Morizet et al. 2017) whereas other experimental data have been interpreted to suggest that oxygen in the CO_3^{2-} complex is shared with the silicate network (Brooker et al. 2001).

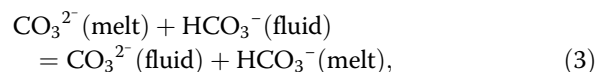
Equation (1) obviously is a simplification. For example, this equation does not account for the observation that the HCO_3/CO_3 abundance ratio in both melts and fluids is temperature dependent (Fig. 3a) From the temperature dependence of the HCO_3/CO_3 abundance ratio in melts and in fluids and under the assumption of ideal mixing, the enthalpy change is 17 ± 3 and 29 ± 9 kJ/mol for melt and fluid, respectively. Equilibrium (1) likely also depends on temperature, and definitely on the activity of CO_2 and protons (pH) but experimental data with which to address such questions have not been reported.

Methane is a stable species in COH fluid under reducing conditions (Kadik et al. 2004). In silicate–COH, this oxidation state was detected with carbon-13 MAS NMR in glasses formed by quenching of melts from 1450 °C and 2 GPa and with f_{H_2} controlled by the magnetite-wüstite– H_2O and more reducing conditions (Mysen et al. 2011). It was, furthermore, noted in the latter study that molecular CH_4 coexists with methyl groups (CH_3) in the melt similar to that more recently also reported by Ardia et al. (2013). Mysen et al. (2011) reported ^{13}C NMR-based evidence that these CH_3 groups were not linked to oxygen (methoxy groups). That conclusion may imply that the methyl groups actually replace oxygen in silicate tetrahedral with an equilibrium between CH_4 , CH_3 and silicate species that in principle can be expressed as:

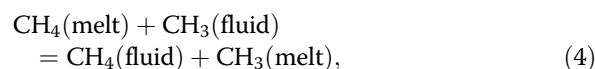


In this equation, the $\text{Q}^n(\text{CH}_3)_2$ notation indicates that two of the n oxygens have been replaced by CH_3 groups.

Even though in silicate–COH systems both HCO_3/CO_3 and CH_3/CH_4 abundance ratios vary in both melts and coexisting fluids, the exchange equilibria for oxidizing conditions (Fig. 3c);



and reducing conditions (Fig. 3d);



are such that under all conditions in Fig. 3, with increasing temperature under oxidizing conditions the CO_3/HCO_3 abundance ratio increases faster in melts than in

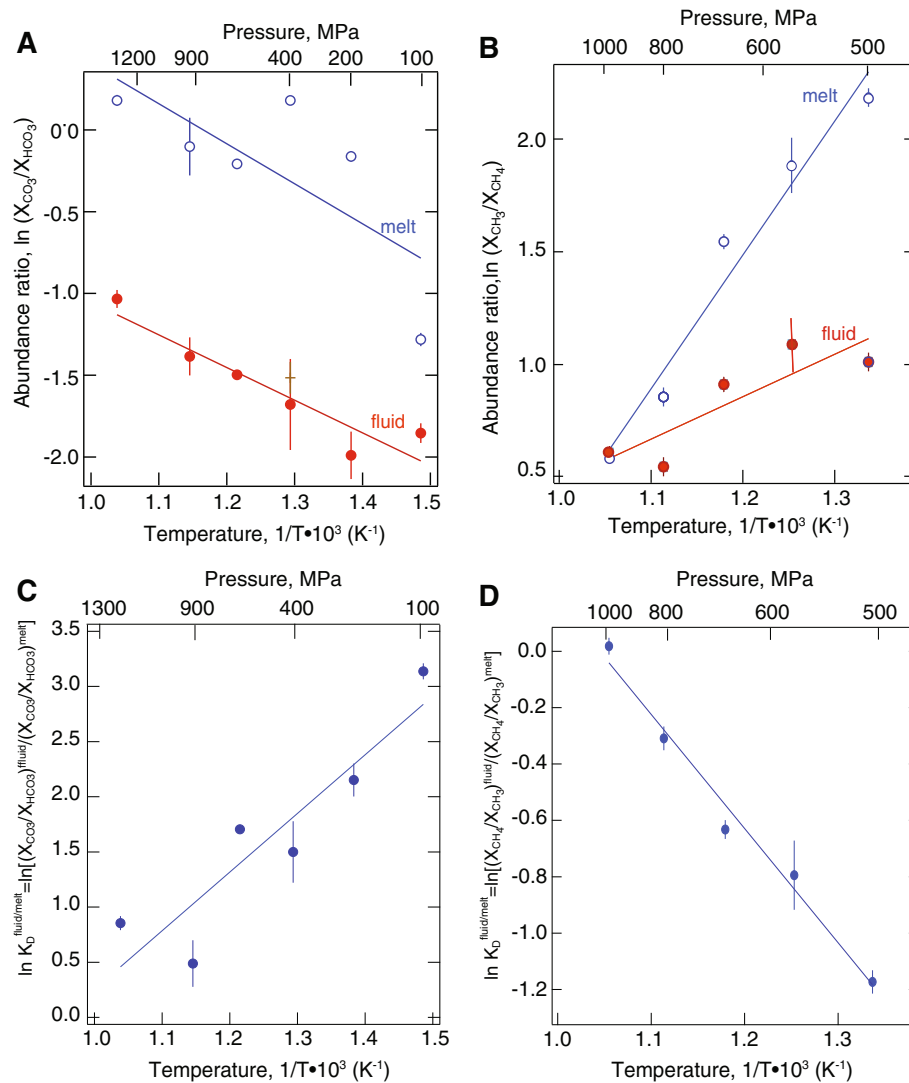


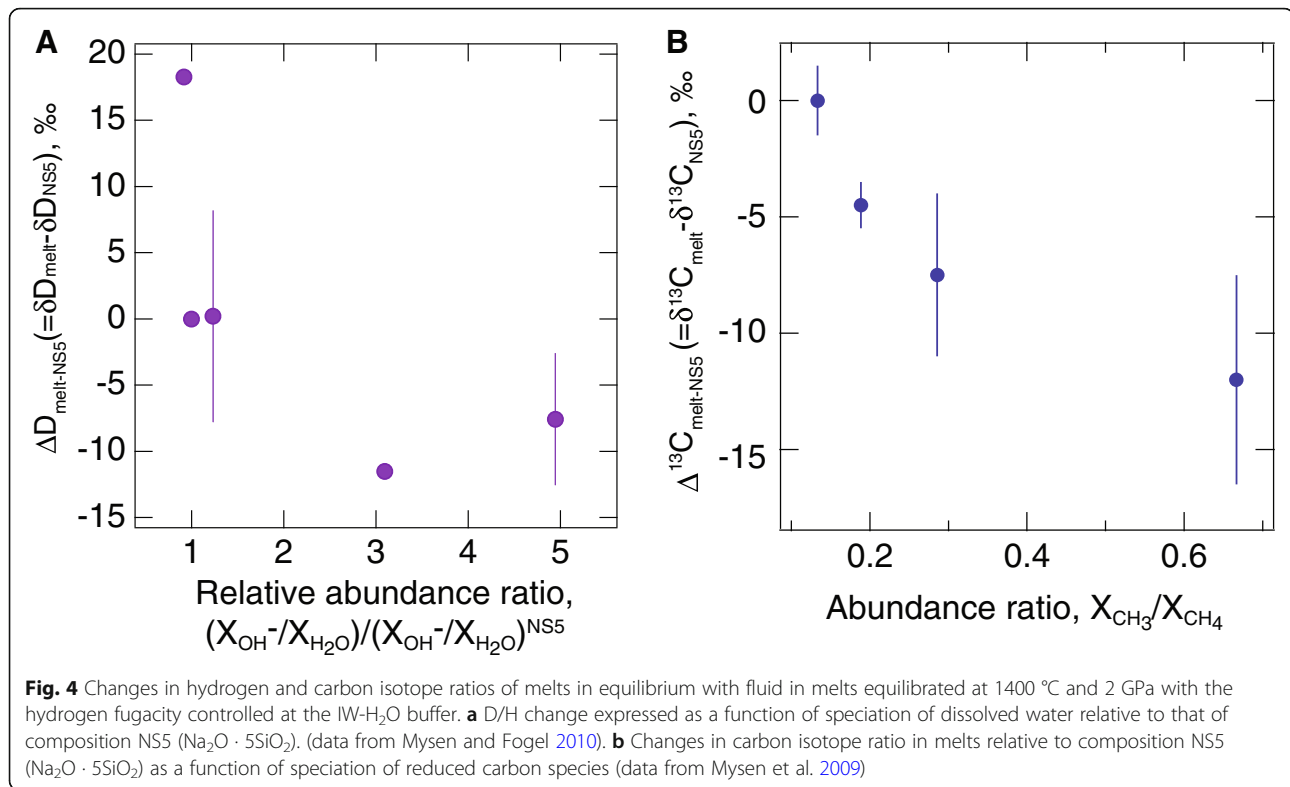
Fig. 3 Abundance of C-bearing species in coexisting COH fluids and melts as a function of temperature and pressure as indicated. **a** Evolution of carbonate species under oxidizing conditions. **b** Evolution of C-bearing species under reducing conditions. **c** Evolution of fluid/melt exchange of carbonate species under oxidizing conditions. **d** Evolution of fluid/melt exchange of C-bearing reduced species under reducing conditions. Note that temperature is the independent variable with pressure evolving as a function of temperature as described briefly in the text and in more detail in the original sources (modified after Mysen 2015a, 2015b). The ΔH values derived from the linear regression of the data are discussed in the text. In calculated these ΔH values, it was assumed that there is no pressure effect on these equilibria

coexisting fluid. The enthalpy change, ΔH , for reaction (3) is -44 ± 9 kJ/mol with the assumption of ideal mixing (Mysen 2015a). Under reducing conditions, the CH_4/CH_3 abundance ratio in fluid increases faster than in coexisting melt with a ΔH for reaction (4) of 34 ± 3 kJ/mol (Mysen 2015b).

Hydrogen and carbon isotope behavior

In a situation where there is no interaction between the molecules, isotope fractionation factors can be calculated (Bigeleisen and Mayer 1947; Bottinga 1968). However, in most magmatic environments, there are indeed interactions between various silicate and COH complexes

(Chacko et al. 2001). Changes in structural complexes in fluids and brines are known to affect isotope behavior (Horita 1988; O'Neil and Truesdell 1993; Horita et al. 1995; O'Neil et al. 2004). Isotope substitution also can affect materials properties (Horita et al. 2010). It should not be surprising, therefore, that significant isotope fractionation can be observed between melts or fluids with variable structural complexes. For example, hydrogen and carbon isotope ratios in melts in equilibrium with fluid of fixed composition vary as a function of changes on solution mechanisms of COH species in the melt (Fig. 4). The data in Fig. 4 were obtained by analyzing glasses along the join $\text{Na}_2\text{O}-\text{SiO}_2$ after quenching from



equilibration with a COH fluid at 1400 °C and 2 GPa and with the hydrogen fugacity buffered with the iron-wüstite-H₂O buffer. Isotope variations are expressed relative to composition, NS5 (Na₂O · 5SiO₂). Subsequent spectroscopic examination of the fluid, which remained of constant composition in all experiments, was a mixture of CH₄, H₂, and H₂O. It can be seen quite clearly that the D/H and ¹³C/¹²C ratios respond to changes in water and methane speciation in the melt, respectively. Similar effects have been reported for D/H fractionation in melts formed in the silicate–H₂O–D₂O systems determined with proton and deuteron MAS NMR (Wang et al. 2015). Analogous experimental data were reported by Dobson et al. (1989) for D/H fractionation between fluid and rhyolite and feldspar melts and Matthey et al. (1990) and Matthey (1991) for carbon isotope fractionation between fluid, basalt, and sodamelilite melt. In light of the more recent data such as summarized in Fig. 4, those earlier data likely reflected variations in speciation of the volatiles in the synthetic and natural melts.

In studies such as those described in the previous paragraph, mass spectrometric measurements were made on glasses and fluids subsequent to quenching from high temperature and pressure. However, fluids quenched from pressures in the GPa pressure range and high temperature such as was the case with those experiments often comprise several molecular silicate components. These silicate-rich fluids are prone to precipitation of solid

materials during quenching. There are also the problems that derive from exsolution of fluid from melts as these are cooled during quenching thus changing the content and possibly proportion of volatile components.

In order to circumvent quenching problems, more recent experiments have combined high-temperature/high-pressure experiments conducted in diamond anvil cells with vibrational spectroscopy as a means to obtain isotope ratios of elements whose isotopic mass differences are relatively large (e.g., D and H, ¹³C and ¹²C; see (Foustoukos and Mysen 2012; Mysen 2013; Dalou et al. 2015).

With this method, it is taken advantage of the fact that vibrational frequencies are discrete functions of oscillator mass:

$$\nu_1 = \nu_2 \cdot \sqrt{\frac{m_1}{m_2}}, \quad (5)$$

where ν_1 and ν_2 are vibrational frequencies of a specific mode for isotopes 1 and 2. The m_1 and m_2 are the atomic masses of the ¹²C and ¹³C oscillator. In the case of an elemental phase such as graphite or diamond, m_1 and m_2 could be ¹²C and ¹³C.

We emphasize that the frequency difference between vibrations with two different isotopes does not change with abundance, but the vibrational intensity, expressed

as integrated areas, A_1 and A_2 , does. From vibrational spectra, the isotope ratio, X_1/X_2 , of a sample then becomes

$$A_1/A_2 = X_1/X_2. \quad (6)$$

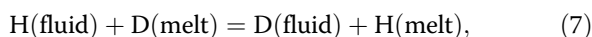
Such vibrational spectroscopic methods have been used to determine hydrogen and carbon isotope ratios in coexisting silicate melts and fluids in silicate–COH systems contained in hydrothermal diamond anvil cells at pressures and temperatures up to those of the Earth's upper mantle. In some of these experiments, redox conditions were controlled with metal/oxide buffers (Re/ReO₂, Ti/TiO₂).

The method has the significant advantage that the analyses are conducted in situ while the samples are the conditions of interest, the method is non-destructive and with spatial resolution on the micrometer scale (see above). There is, therefore, no concern for sample changes during quenching because quenching is not involved. It can also probe quite small samples without interference from adjacent phases. Moreover, in this experimental environment, pressure/temperature conditions can be changed quickly (on the time scale of minutes) without changing the sample. A potential limitation is the sensitivity of the method to isotope abundances relevant to natural conditions. In an effort to assess whether or not this could be a problem, Dalou et al. (2015) conducted experiments with several series of fluid/melt D/H fractionation with different bulk D/H ratios in silicate–H₂O–D₂O systems, but did not find any concentration-dependent variations (Fig. 5).

Hydrogen isotopes

In silicate–COH melt and fluid systems, the principal hydrogen-bearing species are H₂O, OH, H₂, CH₄, CH₃, and HCO₃ where redox conditions and chemical composition of the fluids govern which species will dominate. The molecular species, H₂O and H₂, when present likely occupy 3-dimensional cavities in glass and melts much like that reported for noble gases, for example (Carroll and Stolper 1993; Zhang et al. 2010; Guillot and Sator 2012). Hydrogen isotopes in those molecular species likely will not show significant fractionation effects. As to bicarbonate, HCO₃, no clear isotopic effects in either infrared or Raman spectra (Mysen 2015a) which may suggest that the C–O bond is not affected detectably whether H⁺ or D⁺ forms the bicarbonate complex.

For the exchange equilibrium,



under both oxidizing and reducing conditions, the dominant contribution is via OD/OH fractionation. The

appearance of the vibrational modes assigned to O–D and O–H stretch vibrations is shown in the insert in Fig. 6, where the exchange equilibrium coefficient, $K_{D/H}^{\text{fluid/melt}}$, is defined as;

$$K_{D/H}^{\text{fluid/melt}} = \left[\frac{(D/H)(\text{fluid})}{(D/H)(\text{melt})} \right], \quad (8)$$

where D/H denotes abundance ratio. From experiments conducted under oxidizing conditions, the D/H ratio simply is the ratio of integrated intensity such as indicated in the insert in Fig. 6, whereas for reducing conditions, information from deuterated methane and methyl complexes also is incorporated.

The D/H evolution with temperature in fluids and melts under oxidizing and reducing conditions differ significantly (Table 1). In general, under oxidizing conditions the ΔH is greater, whether in melts or coexisting fluids. The D/H abundance ratio in fluid always is greater than that in melt. This behavior leads to a D/H exchange coefficient that not only differs at given temperature and pressure, but the rate of change with temperature is different under oxidizing and reducing conditions (Fig. 6; see also Table 1). Notably, experimentally determined D/H fractionation data for rhyolite–H₂O and feldspar composition–H₂O (Dobson et al. 1989) are quite similar to those of silicate–COH under reducing conditions (Fig. 6). Furthermore, the temperature-dependent D/H fractionation in silicate–H₂O–D₂O, using the same silicate composition and working in similar temperature and pressure ranges, result in $\Delta H = 6.5 \pm 0.7$ kJ/mol (Mysen 2013). These groups have somewhat similar structural behavior (see discussion above—Eq. (2)) so a closer similarity between silicate–COH under reducing conditions and silicate–H₂O than between silicate–COH under oxidizing conditions and silicate–H₂O may not be so surprising.

The variations of D/H ratios in fluids and melts and, therefore, in the D/H exchange coefficient are because of changing silicate and COH speciation with changing redox conditions (Kadik et al. 2004; Mysen et al. 2011; Ardia et al. 2013). Additionally, speciation change as a function of temperature and pressure takes place partly because silicate solute concentration in the fluid increases and partly because of changing C-bearing species abundance in the melt (Manning 2004; Newton and Manning 2008; Mysen et al. 2009; Mibe and Bassett 2008; Mysen et al. 2013). Network-modifying cations, which include H⁺ and D⁺ (which form bonding with nonbridging oxygen), will show preference for specific silicate species depending on the ionization potential of the metal cation as has been demonstrated with ¹H and ²H MAS NMR spectroscopy (Wang et al. 2015). These

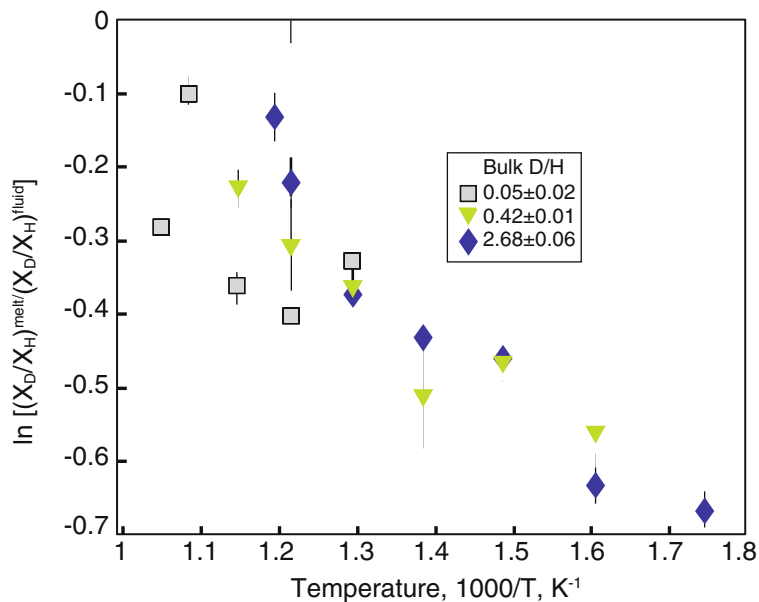


Fig. 5 D/H exchange equilibrium coefficient between coexisting fluid and melt in silicate–H₂O as a function of temperature and bulk D/H abundance ratio (data from Dalou et al. 2015)

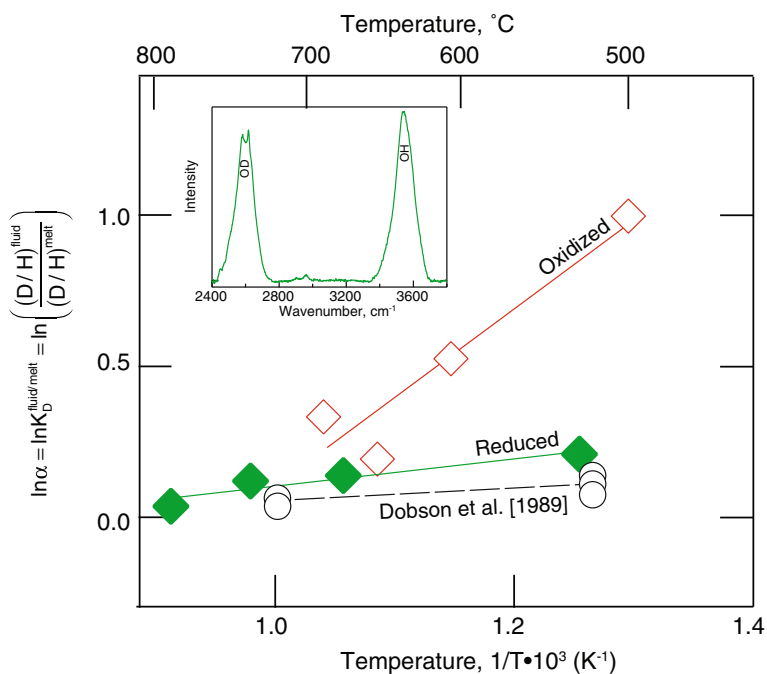


Fig. 6 Fractionation factor, α , set equal to the fluid/melt exchange equilibrium coefficient (see text for discussion) for D/H exchange between coexisting fluid and melt as a function of temperature in silicate–COH systems under reducing and oxidizing conditions. Insert shows typical Raman spectrum (here from fluid) to illustrate the appearance of the Raman bands assigned to OD and OH stretch vibrations and used to extract the data themselves. The ΔH values from the two fits are given in Table 1. Also shown are the experimental data for rhyolite–H₂O and feldspar–D₂O glass and melt composition in the 5–20 MPa pressure range from Dobson et al. (1989) (data otherwise from Mysen 2015a)

Table 1 Enthalpy of D/H fractionation in coexisting fluid and melt in silicate-COH under oxidizing and reducing conditions (data from Mysen 2015a)

	Oxidizing	Reducing
$\Delta H(\text{fluid})^*$	9.7 ± 2.0 kJ/mol	-4.9 ± 1.1 kJ/mol
$\Delta H(\text{melt})^*$	34 ± 4 kJ/mol	-1.2 ± 0.2 kJ/mol
$\Delta H(\text{Eq. 8})^{**}$	24.8 ± 6 kJ/mol	-4.5 ± 0.5 kJ/mol

In all cases, ideal mixing is assumed

*Enthalpy change from temperature-dependent D/H abundance ratio, $\ln(X_{\text{OD}}/X_{\text{OH}})$ vs. $1/T$ (K^{-1}), in fluid and melt

** Enthalpy change from temperature-dependent exchange equilibrium coefficient between fluid and melt, $\ln[(X_{\text{OD}}/X_{\text{OH}})^{\text{fluid}}/(X_{\text{OD}}/X_{\text{OH}})^{\text{melt}}]$ vs. $1/T$ (K^{-1})

effects govern H^+ - and D^+ -oxygen bonding, with the temperature (and pressure)-dependent D/H ratio summarized in Fig. 6 as the result.

D/H behavior in COH-fluid-saturated magmatic systems

Variations in COH speciation in silicate-COH systems at high temperature and pressure affect melt polymerization. Silicate speciation and melt polymerization affect all physical and chemical properties of magmatic liquids, including D/H fractionation among species in the phases (Wang et al. 2015) which, in turn, will affect melt/mineral/fluid D/H fractionation behavior. This feature is evident in Fig. 6. Both redox conditions and abundance of COH volatiles are important.

Experimental data such as summarized in Fig. 6 (see also Table 1) can be employed to illustrate how temperature and redox conditions affect D/H fractionation factors, $\alpha_{\text{D/H}}^{\text{fluid/melt}}$, and how the fractionation factors, in turn, influence D/H evolution of melts and fluids in magmatic silicate-COH systems in the upper mantle and the deep crust. In doing this, I emphasize, however, that the data to be used are from model compositions in the $\text{Na}_2\text{O}-\text{Al}_2\text{O}_3-\text{SiO}_2-\text{COH}$ system and should, therefore, not be applied quantitatively to natural magmatic processes. The behavior does, however, illustrate principles that should be kept in mind when applying hydrogen isotope data to deduce petrogenetic processes in the Earth's interior.

The exchange equilibrium coefficient, $K_{\text{D/H}}^{\text{fluid/melt}}$, in Eq. (8) equals the D/H fraction factor, of $\alpha_{\text{D/H}}^{\text{fluid/melt}}$, provided that the $K_{\text{D/H}}^{\text{fluid/melt}}$ is independent of bulk composition. According to the results in Fig. 5, this seems a reasonable assumption. Then, we can write its temperature-dependence;

$$\ln K_{\text{D/H}}^{\text{fluid/melt}} = \ln \alpha_{\text{D/H}}^{\text{fluid/melt}} = a/T + b, \quad (9)$$

where T is temperature (kelvin) and a and b are the regression coefficients in a plot such in Fig. 6. The fractionation factor is a strong non-linear function of temperature and is more sensitive to temperature under

oxidizing conditions than under reducing conditions (Fig. 7). That fact that these curves do indeed pass through 1 as the result of changing silicate content in the fluid and COH fluid content in the melt with increasing temperature.

As an example of how the D/H relationships may affect the D/H evolution of magmatic liquids in (COH)-bearing mantle environments, let us start with the assumption that the COH fluid retains a fixed D/H = ratio, δD , of -100% . This value was chosen because it is reasonable near the δD value range of the Earth's upper mantle (Bell and Ihinger 2000). The δD values of the melt in equilibrium with such a fluid is

$$\delta D^{\text{melt}} = \frac{\delta D^{\text{fluid}}}{\alpha_{\text{D/H}}^{\text{fluid/melt}}} + 1000 \cdot \frac{1 - \alpha_{\text{D/H}}^{\text{fluid/melt}}}{\alpha_{\text{D/H}}^{\text{fluid/melt}}}. \quad (10)$$

In Eq. (10), $\alpha_{\text{D/H}}^{\text{fluid/melt}}$ is defined in Eq. (9).

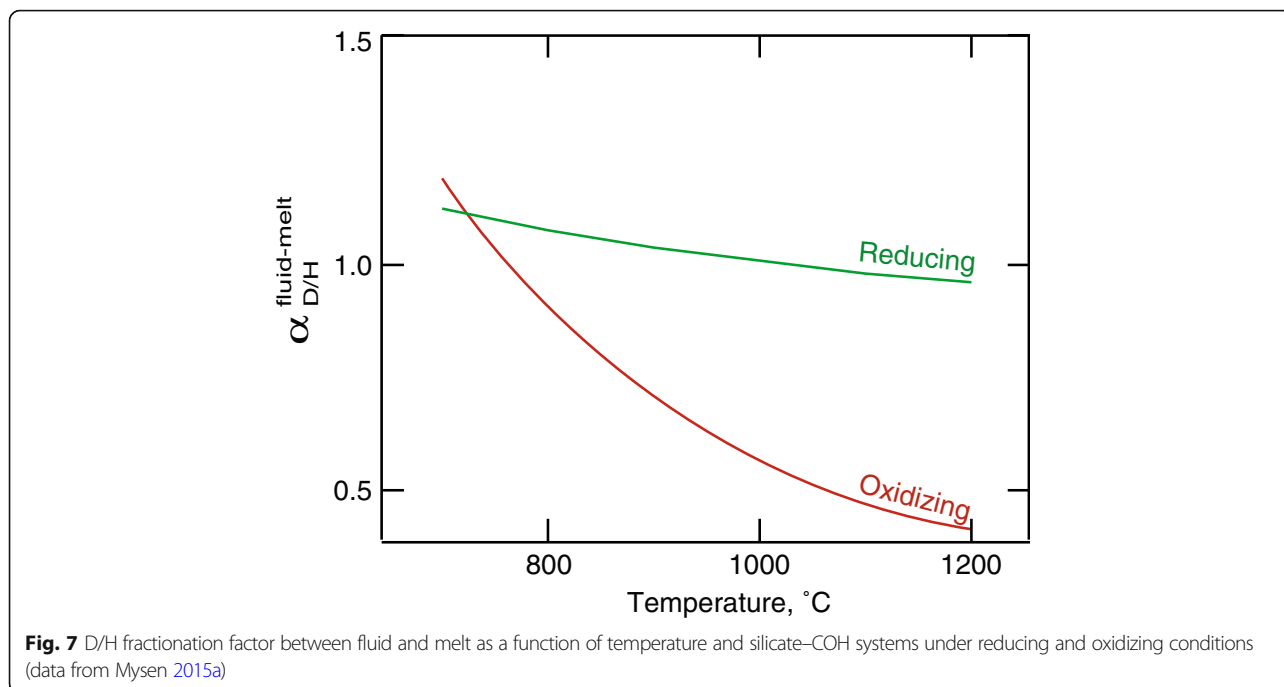
As can be seen from the calculated results (Fig. 8), this leads to the suggestion that a magmatic liquid in equilibrium with COH fluid under oxidizing conditions can be as much as 100% heavier than a melt equilibrated with COH under reducing conditions. The δD^{melt} difference is not significantly dependent on temperature of equilibration.

Carbon isotopes

For carbon isotopes, ^{13}C and ^{12}C , the relationship between vibrational frequency and oscillator mass in Eq. (5) would suggest a frequency difference near 4% if the masses simply were those of the carbon isotopes. However, this is not the case. For oxidized carbon, the frequency shift of C-O stretch vibrations, which for natural carbon (nearly pure ^{12}C) occur near 1070 cm^{-1} in the Raman spectra (Frantz 1998) is only about 1.5%. Under reducing conditions, that of C-H stretch vibrations is less than 1% (see inserts in Fig. 9). This happens because oxygen and hydrogen vibrations, respectively, contribute to the oscillator mass.

In an examination of carbon isotope behavior in silicate-COH systems under oxidizing conditions, the behavior of both CO_3^{2-} and HCO_3^- complexes and their linkage to the silicate structure in fluids and melts need to be addressed (see Eq. (1)). This is so because the $^{13}\text{C}/^{12}\text{C}$ ratio and its temperature-dependence in coexisting CO_3^{2-} and HCO_3^- differ (Table 2).

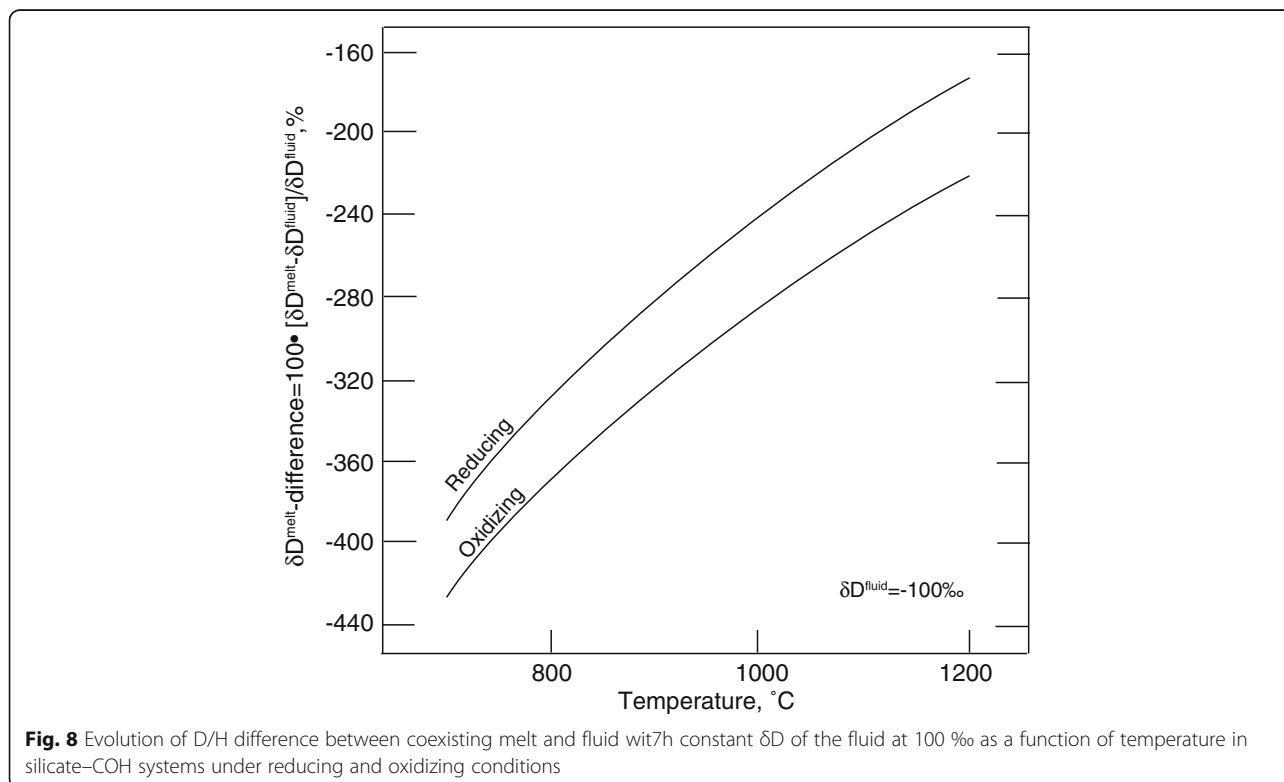
The variations with temperature of the $^{13}\text{C}/^{12}\text{C}$ ratios in the CO_3 and HCO_3 species also differ in fluids and melts (Table 2). In fluid, the $^{13}\text{C}/^{12}\text{C}$ ratio in HCO_3 species decreases with temperature (and pressure) whereas for the CO_3 groups, the opposite temperature trend is observed (Table 2). For (C-O-H)-saturated melt coexisting with fluid, on the other

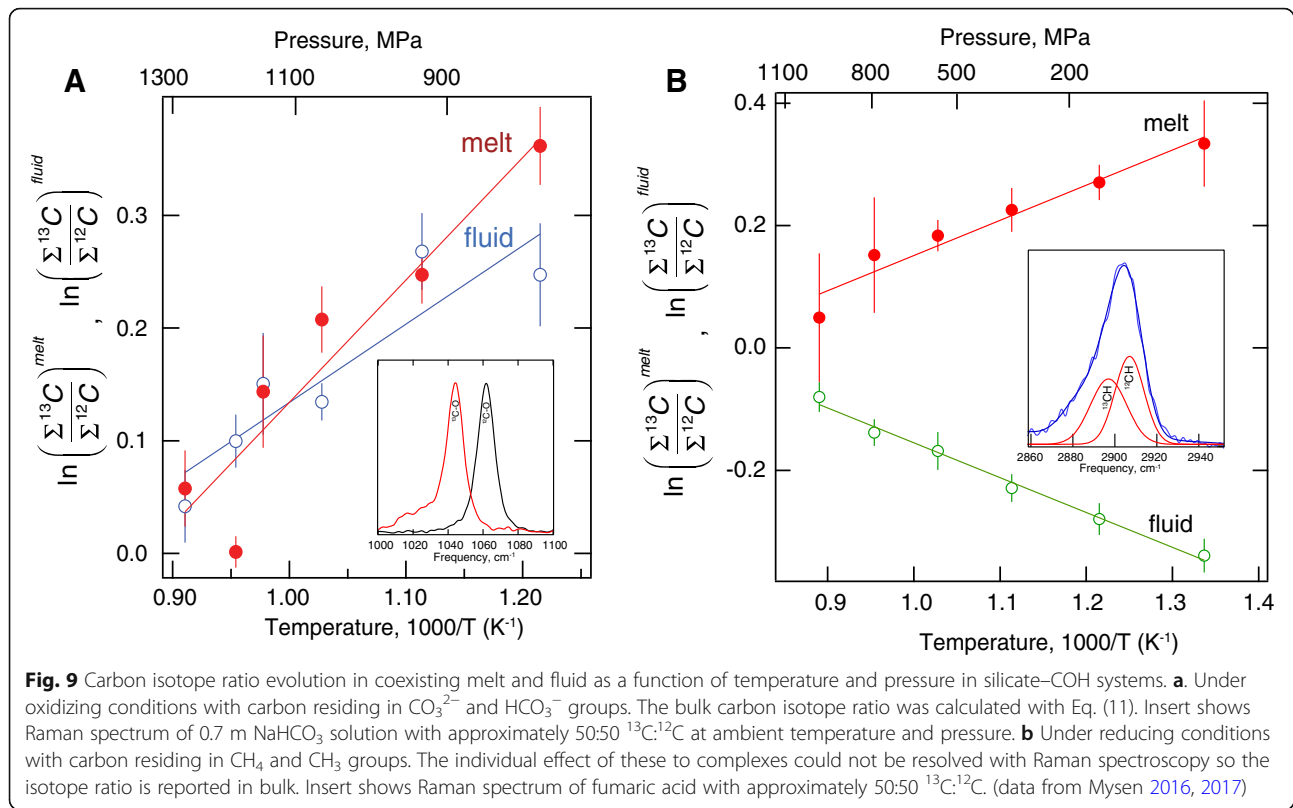


hand, the $^{13}\text{C}/^{12}\text{C}$ ratio of HCO_3 complexes increases and that of CO_3 complexes decreases with increasing temperature and pressure (Table 2). The absolute ΔH values for carbonate complex variations in melts is greater than for fluids, but do, of course, approach

one another as the temperature (825 °C) and pressure (1303 MPa) conditions of supercritical phase stability field are reached (Mysen 2017).

The different temperature trajectories of the $^{13}\text{C}/^{12}\text{C}$ in fluids and melts probably reflect the much





higher silicate and aluminosilicate content of melts compared with fluid. This difference is responsible for the presence of essentially only Q^0 species in fluids compared with significant abundance of more polymerized aluminosilicate species in the melt (Mysen

Table 2 Enthalpy of $^{13}\text{C}/^{12}\text{C}$ fractionation in coexisting fluid and melt in silicate–COH under oxidizing and reducing conditions (data from Mysen 2016, 2017)

Oxidizing	Reducing
$\Delta\text{H}_{\text{CO}_3(\text{fluid})}^*$	$\Delta\text{H}_{\text{CH}_4(\text{fluid})}^\dagger$
$\Delta\text{H}_{\text{HCO}_3(\text{fluid})}^{**}$	$\Delta\text{H}_{\text{CH}_4(\text{melt})}^\ddagger$
$\Delta\text{H}_{\text{CO}_3(\text{melt})}^*$	$\Delta\text{H}_{\text{K}_{\text{melt}/\text{fluid}}}^b$
$\Delta\text{H}_{\text{HCO}_3(\text{melt})}^{**}$	
$\Delta\text{H}_{\Sigma^{13}\text{C}/\Sigma^{12}\text{C}(\text{melt})}^a$	
$\Delta\text{H}_{\Sigma^{13}\text{C}/\Sigma^{12}\text{C}(\text{fluid})}^a$	
$\Delta\text{H}_{\text{K}_{\text{melt}/\text{fluid}}}^b$	

* $\Delta\text{H}_{\text{CO}_3(\text{fluid})}$ and $\Delta\text{H}_{\text{CO}_3(\text{melt})}$ were derived from the relationship, $\ln(^{13}\text{C}/^{12}\text{C})$ vs. $1/T$ (K^{-1}) in fluid and melt under oxidizing conditions

** $\Delta\text{H}_{\text{HCO}_3(\text{fluid})}$ and $\Delta\text{H}_{\text{HCO}_3(\text{melt})}$ were derived from the relationship, $\ln(^{13}\text{C}/^{12}\text{C})$ vs. $1/T$ (K^{-1}) in fluid and melt under oxidizing conditions

† $\Delta\text{H}_{\text{CH}_4(\text{fluid})}$ and $\Delta\text{H}_{\text{CH}_4(\text{melt})}$ were derived from the relationship, $\ln(^{13}\text{C}/^{12}\text{C})$ vs. $1/T$ (K^{-1}) in fluid and melt under reducing conditions

^aThe same as for $\Delta\text{H}_{\text{CO}_3(\text{fluid})}$ and $\Delta\text{H}_{\text{CO}_3(\text{melt})}$ except that total carbonate ratio $\Sigma^{13}\text{C}/\Sigma^{12}\text{C}$, where total carbonate is $\text{CO}_3 + \text{HCO}_3$, is used

^b $\Delta\text{H}_{\text{K}_{\text{melt}/\text{fluid}}}$ under oxidizing and reducing conditions was derived from the relationship, $\ln[(\Sigma^{13}\text{C}/\Sigma^{12}\text{C})^{\text{melt}}/(\Sigma^{13}\text{C}/\Sigma^{12}\text{C})^{\text{fluid}}]$ vs. $1/T$ (K^{-1})

2017). Given the interaction between the carbonate groups and oxygen in the Q-species in the melts and the fact that nonbridging oxygen in Q-species of different degree of polymerization likely are energetically diggerent (Kohn and Schofield 1994; Mysen 2007), it follows that the energetics of oxygen bonds associated with CO_3 and HCO_3 groups is also different. These difference, in turn, means that energetics of the C–O bonds in CO_3 and HCO_3 groups differ. As a result, the $^{13}\text{C}/^{12}\text{C}$ abundance evolution with temperature (and pressure) of these groups in silicate melt will differ from that in fluid. These differences in silicate speciation in fluid and melt change, however, with temperature and pressure. In particular, the silicate content of the fluid likely increases, which will cause changes in Q-speciation in the fluid (Mysen et al. 2013). As this occurs, the influence of fluid composition on its $^{13}\text{C}/^{12}\text{C}$ ratio will also become increasingly important, a conclusion which is similar to that made for temperature- and pressure-dependent changes D/H fractionation in silicate– H_2O and silicate–C–O–H systems (Wang et al. 2015; Dalou et al. 2015; Le Losq et al. 2016).

The bulk $^{13}\text{C}/^{12}\text{C}$, $\Sigma^{13}\text{C}/\Sigma^{12}\text{C}$, comprises the contributions from both the CO_3^{2-} and HCO_3^- groups, $^{13}\text{CO}_3^{2-}$, $^{12}\text{CO}_3^{2-}$, $^{13}\text{HCO}_3^-$, and $^{12}\text{HCO}_3^-$ together

with the molecular fraction of the species, X_{CO_3} and $X_{\text{HCO}_3^-}$, where $X_{\text{HCO}_3^-} = 1 - X_{\text{CO}_3}$, so that

$$K_D^{\text{melt}} = \left(\frac{\sum^{13\text{C}}}{\sum^{12\text{C}}} \right)^{\text{melt}} = \left(\frac{X_{\text{CO}_3} g_{13\text{CO}_3^{2-}} + (1 - X_{\text{CO}_3}) g_{13\text{HCO}_3^-}}{X_{\text{CO}_3} g_{12\text{CO}_3^{2-}} + (1 - X_{\text{CO}_3}) g_{12\text{HCO}_3^-}} \right)^{\text{melt}}, \quad (11)$$

and with a similar expression for fluid. The K_D^{melt} and K_D^{fluid} differ (Fig. 9a; Table 2) because the values and temperature-dependence of $^{13}\text{C}/^{12}\text{C}$ of fluid and melt differ.

Therefore, for the carbon isotope exchange equilibrium between melt and fluid under oxidizing conditions we have the exchange equilibrium

$$\sum 12\text{C}(\text{melt}) + \sum 13\text{C}(\text{fluid}) = \sum 12\text{C}(\text{fluid}) + \sum 13\text{C}(\text{melt}). \quad (12)$$

for which,

$$K_D^{\text{melt}/\text{fluid}} = \frac{K_D^{\text{melt}}}{K_D^{\text{fluid}}}, \quad (13)$$

where K_D^{melt} and K_D^{fluid} are defined in Eq. (11) for melt and fluid, respectively.

The temperature-dependence of this $K_D^{\text{melt}/\text{fluid}}$ (Fig. 10b) leads to $\Delta H = 9.5 \pm 0.8$ kJ/mol. Under the assumption that the carbon isotope ratio is not dependent on total carbon concentration, the $K_D^{\text{fluid}/\text{melt}}$ values equal the fractionation factors. The carbon isotope fractionation factor under reducing conditions is about three times as sensitive to temperature than under oxidizing conditions. This means the carbon isotope behavior also differs from the D/H fractionation behavior where oxidizing conditions are those under which the D/H fractionation factor is the most sensitive to temperature.

Carbon isotope behavior in COH-fluid-saturated magmatic systems

Before addressing an example of how redox conditions during melting and crystallization may affect the carbon isotope behavior, the reader is reminded that the data to be used for this illustration were obtained in simple three component systems and with only one C/O/H ratio of the fluid component. We must also remember that the melts examined in this study were (C–O–H)-saturated and the coexisting (C–O–H) fluids were silicate-saturated. The speciation behavior is not, therefore, the same as in silicate-free carbonate–H₂O system

such as in the in situ studies of Facq et al. (2014) and Foustoukos and Mysen (2015).

The example below, therefore, is intended to illustrate principles, but not necessarily quantitative behavior. Calculated $\delta^{13}\text{C}$ -evolutions in a melt in equilibrium with a (C–O–H)-bearing source with $\delta^{13}\text{C}$ of fixed at -7 and -30 ‰ and in a temperature corresponding to those of magmatic processes in the deep crust and upper mantle are shown in Fig. 11. The -7 and -30 ‰ $\delta^{13}\text{C}$ values correspond to the range in $\delta^{13}\text{C}$ of mantle-derived peridotite and eclogite nodules in basalt and kimberlite (see Deines 2002, for review).

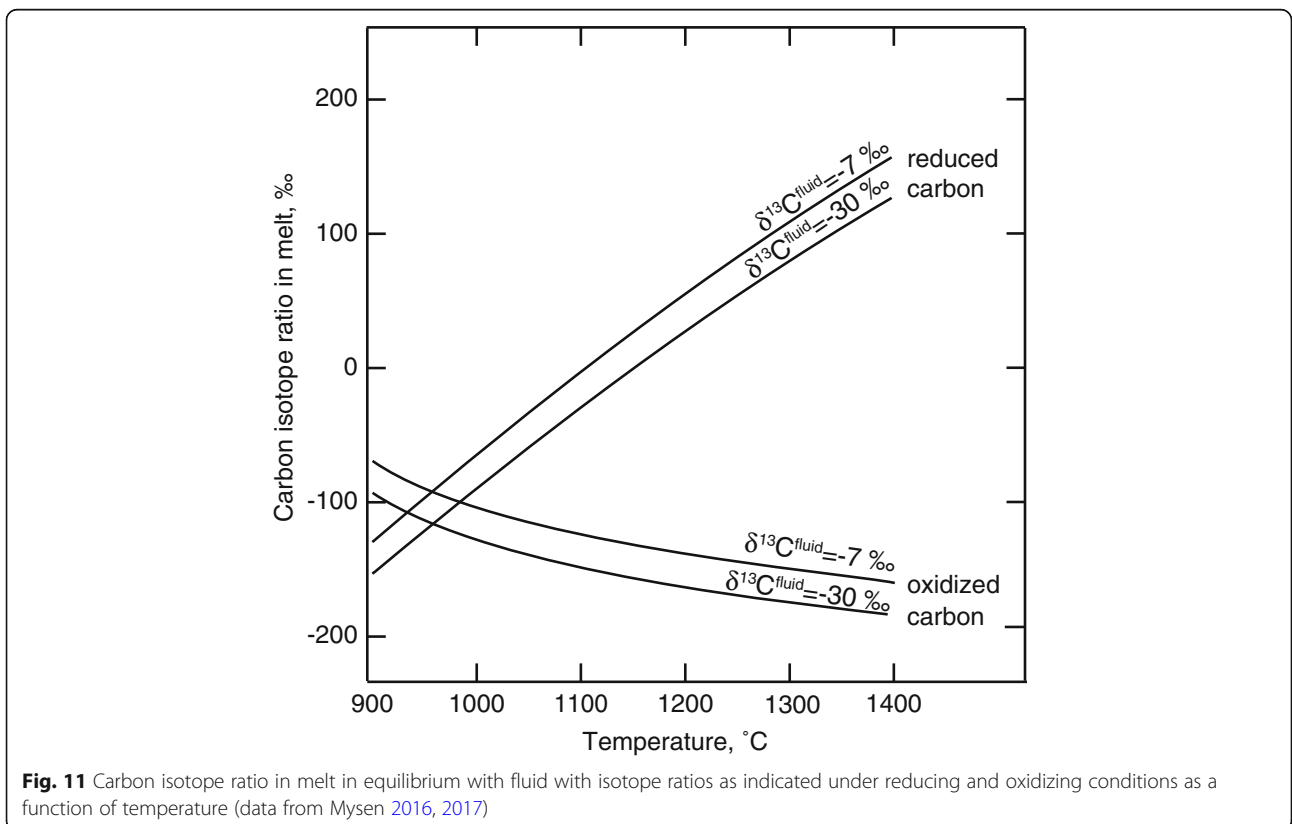
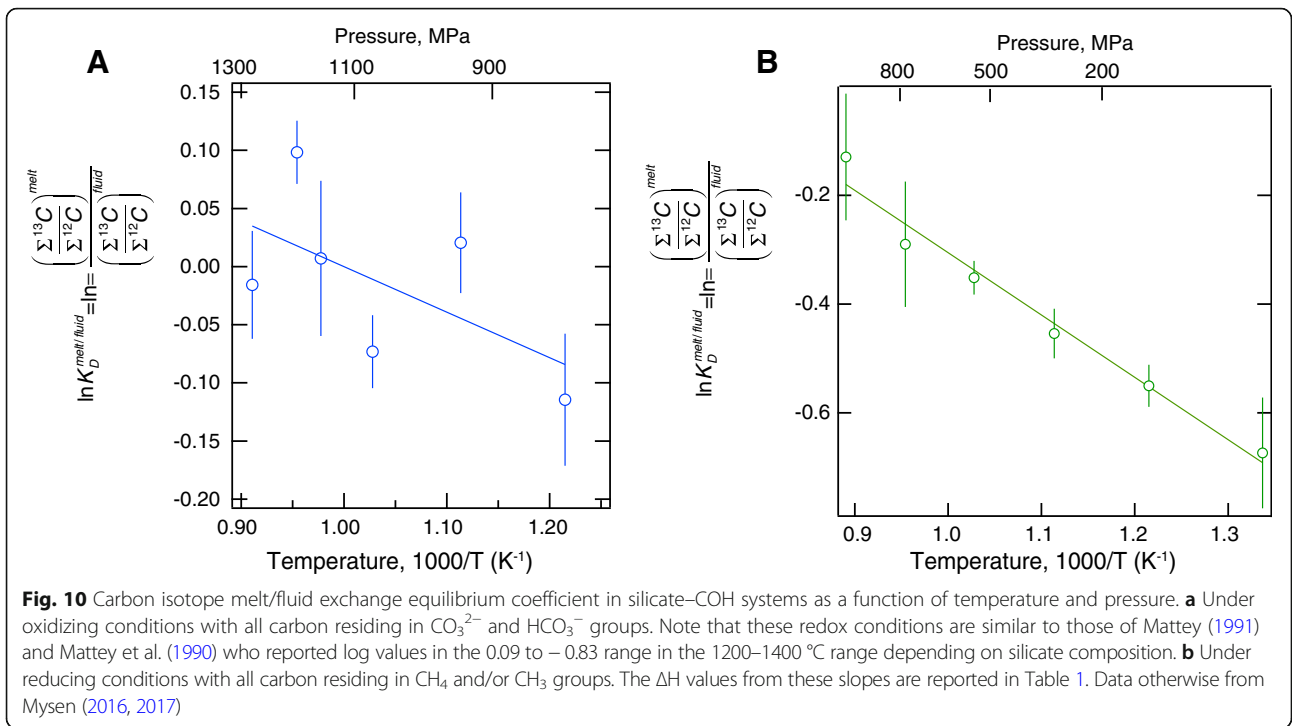
For a melt, its $\delta^{13}\text{C}$ value can differ from that of the source region by more than 100‰ and this difference increases with increasing temperature (Fig. 11). This also means that exsolution of C–O–H fluid from a melt in the upper mantle and deep crust, the $\delta^{13}\text{C}$ of an evolving CO₂-rich fluid can be equally enriched in carbon-13 relative to the magma. This isotope behavior is, however, quite different under reducing and oxidizing conditions regardless of the $\delta^{13}\text{C}$ value of the source rock (Fig. 11). Under reducing conditions, (COH)-saturated melts are isotopically heavier than silicate-saturated fluids. Under oxidizing conditions, the $\delta^{13}\text{C}$ of the magmatic liquid at lower temperature is also heavier than fluid, but the temperature effect shifts this value to become isotopically lighter at higher temperature. This different behavior under reducing and oxidizing conditions reflects the different structural roles and effects on melt and fluid structure depending on the oxidation state of carbon (Mysen 2015a) (see also Eqs. (1) and (2)). It follows that changing redox conditions during melting and crystallization of (C–O–H)-bearing deep crust and upper mantle can have profound effect on the carbon isotopic signature of the melt.

Conclusions

The behavior of COHN fluids, their isotopes, and their interaction with magmatic liquids are at the core of understanding formation and evolution of the Earth.

The solubility of individual COHN components in silicate melts can differ by several orders of magnitude and ranges from several hundred ppm to several wt% at upper mantle pressure and temperature. Silicate solubility in fluid can reach several molecular. Different solubility of oxidized and reduced C-bearing species in melts reflects different solution equilibria. The oxidized species are H₂O, OH⁻, CO₃²⁻, HCO₃⁻, CO₂, and N₂, whereas reduced species are H₂O, OH⁻, H₂, CH₄, CH₃, NH₃, and NH₂. The C-solubility decreases and N-solubility increases with f_{O_2} below the QFM oxygen buffer.

The structural changes with variable redox conditions of carbon and silicate in magmatic melts and fluids result in D/H, $^{13}\text{C}/^{12}\text{C}$, and $^{15}\text{N}/^{14}\text{N}$ fractionation between



melt, fluid, and crystalline materials that depend on redox conditions and can differ significantly from 1 even at magmatic temperatures. The D/H fractionation between aqueous fluid and magma yields ΔH between -5 and 25 kJ/mol depending on redox conditions. The ΔH values for $^{13}\text{C}/^{12}\text{C}$ fractionation factors are near -3.2 and 1 kJ/mol under oxidizing and reducing conditions, respectively. These differences are because energetics of O–D, O–H, O– ^{13}C , and O– ^{12}C bonding environments are governed by different solution mechanisms in melts and fluids.

It is suggested that (COH)-saturated partial melts in the upper mantle can have δD values of 100‰, or more, lighter than coexisting silicate-saturated fluid. This effect is greater under oxidizing than under reducing conditions. Analogous relationships exist for $^{13}\text{C}/^{12}\text{C}$. For example, at magmatic temperatures in the Earth's upper mantle, $^{13}\text{C}/^{12}\text{C}$ of melt in equilibrium with COH-bearing mantle in the -7 to -30 ‰ range increases with temperature from about 40 to >100 ‰ and 80–120 ‰ under oxidizing and reducing conditions, respectively.

Acknowledgements

Instrument, electronics, and library support was provided by Geophysical Laboratory technical staff. Two reviewers of the manuscript are gratefully acknowledged.

Funding

The research in this review was supported in by grants EAR-1212754, EAR-1250449, and EAR-0707861 from the National Science Foundation.

Availability of data and materials

This is a review paper. All data discussed here are in the original papers cited in the text.

Authors' contributions

All research of the manuscript was by the author. All authors read and approved the final manuscript.

Competing interests

The authors declare that they have no competing interests.

Publisher's Note

Springer Nature remains neutral with regard to jurisdictional claims in published maps and institutional affiliations.

Received: 22 May 2018 Accepted: 13 August 2018

Published online: 01 September 2018

References

- Aranovich LY, Newton RC (1999) Experimental determination of $\text{CO}_2\text{-H}_2\text{O}$ activity-composition relations at 600–1000°C and 6–14 kbar by reversed decarbonation and dehydration reactions. *Am Mineral* 84:1319–1332
- Arculus RJ (1994) Aspects of magma genesis in arcs. *Lithos* 33:189–208
- Ardia P, Hirschmann MM, Withers AC, Stanley BD (2013) Solubility of CH_4 in a synthetic basaltic melt, with applications to atmosphere-magma ocean-core partitioning of volatiles and to the evolution of the Martian atmosphere. *Geochim Cosmochim Acta* 114:52–71. <https://doi.org/10.1016/j.gca.2013.03.028>
- Armstrong LS, Hirschmann MM, Stanley BD, Falksen EG, Jacobsen SD (2015) Speciation and solubility of reduced C–O–H–N volatiles in mafic melt: implications for volcanism, atmospheric evolution, and deep volatile cycles in the terrestrial planets. *Geochim Cosmochim Acta* 171:283–302. <https://doi.org/10.1016/j.gca.2015.07.007>
- Baker MB, Stolper EM (1994) Determination of high-pressure mantle melts using diamond aggregates. *Geochim Cosmochim Acta* 58:2811–2828
- Bassett, W. A., T.-C. Wu, I.-M. Chou, T. Haselton, J. D. Frantz, B. O. Mysen, W.-L. Huang, S. K. Sharma, Schiferl, D. (1996) The hydrothermal diamond anvil cell (DAC) and its applications, in *Mineral Spectroscopy: a Tribute to Roger G. Burns*, edited by M. D. Dyar, C. A. McCammon and M. Schaefer, pp. 261–272, The Geochemical Society, Houston.
- Behrens H, Misiti V, Freda C, Vetere F, Botcharnikov RE, Scarlato P (2009) Solubility of H_2O and CO_2 in ultrapotassic melts at 1200 and 1250 degrees C and pressure from 50 to 500 MPa. *Am Mineral* 94(1):105–120. <https://doi.org/10.2138/am.2009.2796>
- Behrens H, Ohlhorst S, Holtz F, Champenois M (2004) CO_2 solubility in dacitic melts equilibrated with $\text{H}_2\text{O-CO}_2$ fluids: implications for modeling the solubility of CO_2 in silicic melts. *Geochim Cosmochim Acta* 68(22):4687–4703. <https://doi.org/10.1016/j.gca.2004.04.019>
- Behrens H, Roux J, Neuville DR, Siemann M (2006) Quantification of dissolved H_2O in silicate glasses using confocal microRaman spectroscopy. *Chem Geol* 229(1–3):96–112. <https://doi.org/10.1016/j.chemgeo.2006.01.014>
- Behrens H, Yamashita Y (2008) Water speciation in hydrous sodium tetrasilicate and hexasilicate melts: constraint from high temperature NIR spectroscopy. *Chem Geol* 256(3–4):306–315. <https://doi.org/10.1016/j.chemgeo.2008.06.053>
- Bell DR, Ihinger PD (2000) The isotopic composition of hydrogen in nominally anhydrous mantle minerals. *Geochim Cosmochim Acta* 64:2109–2118
- Bigeleisen J, Mayer MG (1947) Calculation of equilibrium constants for isotopic exchange reactions. *J Chem Phys* 15:261–267
- Botcharnikov RE, Behrens H, Holtz F (2006) Solubility and speciation of C–O–H fluids in andesitic melt at $T=1100\text{--}1300$ degrees C and $P=200$ and 500MPa. *Chem Geol* 229(1–3):125–143. <https://doi.org/10.1016/j.chemgeo.2006.01.016>
- Bottinga Y (1968) Calculation of fractionation factors for carbon and oxygen isotopic exchange in the system calcite-carbon dioxide-water. *J Phys Chem A* 72:800–808
- Brooker RA, Kohn SC, Holloway JR, McMillan PF (2001) Structural controls on the solubility of CO_2 in silicate melts Part II: IR characteristics of carbonate groups in silicate glasses. *Chem Geol* 174(1–3):241–254. [https://doi.org/10.1016/S0009-2541\(00\)00318-1](https://doi.org/10.1016/S0009-2541(00)00318-1)
- Carroll MR, Stolper EM (1993) Noble gas solubilities in silicate melts and glasses: new experimental results for argon and the relationship between solubility and ionic porosity. *Geochim Cosmochim Acta* 57(23–24):5039–5052
- Chacko T, Cole DR, Horita J (2001) Equilibrium oxygen, hydrogen, and carbon isotope fractionation factors applicable to geologic systems. In: Valley JW, Cole DR (eds) *Stable isotope fractionation*. Mineralogical Society of America, Washington DC, pp 1–81
- Cody GD, Mysen BO, Lee SK (2005) Structure vs. composition: a solid state ^1H and ^{29}Si NMR study of quenched glasses along the $\text{Na}_2\text{O-SiO}_2\text{-H}_2\text{O}$ join. *Geochim Cosmochim Acta* 69:2373–2384
- Dalou C, Le Losq C, Mysen BO (2015) In situ study of the fractionation of hydrogen isotopes between aluminosilicate melts and coexisting aqueous fluids at high pressure and high temperature - implications for the delta D in magmatic processes. *Earth Planet Sci Lett* 426:158–166. <https://doi.org/10.1016/j.epsl.2015.06.032>
- Deines P (2002) The carbon isotope geochemistry of mantle xenoliths. *Earth Sci Rev* 58:247–278
- Dixon JE, Leist L, Langmuir C, Schilling J-G (2002) Recycled dehydrated lithosphere observed in plume-influenced mid-ocean-ridge basalt. *Nature* 420:385–389
- Dobson PF, Epstein S, Stolper, EM (1988) Hydrogen isotope fractionation between coexisting vapor and silicate glasses and melts at low pressure. In: Anonymous (Ed.), *Geological Society of America, 1988 centennial celebration*. Geological Society of America (GSA), Boulder, p. 190.
- Dobson PF, Epstein S, Stolper EM (1989) Hydrogen isotope fractionation between coexisting vapor and silicate glasses and melts at low pressure. *Geochim Cosmochim Acta* 53:2723–2731
- Eggler DH (1975) Peridotite-carbonate relations in the system $\text{CaO-MgO-SiO}_2\text{-CO}_2$, Carnegie Institution of Washington, Year Book, 74, pp 468–474
- Eggler DH, Baker DR (1982) Reduced volatiles in the system C–H–O: implications to mantle melting, fluid formation and diamond genesis. In: Reidel D (ed) *High-pressure research in geophysics*. Kluwer Academic Publishers, Boston / Dordrecht, pp 237–250
- Eggler DH, Kushiro I, Holloway JR (1979) Free energies of decarbonation reactions at mantle pressures; I, stability of the assemblage forsterite-

- enstatite-magnesite in the system MgO-SiO₂-CO₂-H₂O to 60 kbar. *Am Mineral* 64(3–4):288–293
- Facq S, Daniel I, Montagnac G, Cardon H, Sverjensky DA (2014) In-situ Raman study and thermodynamic model of aqueous carbonate speciation in equilibrium with aragonite under subduction zone conditions. *Geochim Cosmochim Acta* 132:375–390
- Foley SF, Yaxley GM, Rosenthal A, Buhre S, Kiseeva ES, Rapp RP, Jacob DE, E D (2009) The composition of near-solidus melts of peridotite in the presence of CO₂ and H₂O between 40 and 60 kbar. *Lithos* 112:274–283. <https://doi.org/10.1016/j.lithos.2009.03.020>
- Foustoukos DI, Mysen BO (2012) D/H isotopic fractionation in the H₂-H₂O system at supercritical water conditions: composition and hydrogen bonding effects. *Geochim Cosmochim Acta* 86:88–102
- Foustoukos DI, Mysen BO (2015) The structure of water-saturated carbonate melts. *Am Mineral* 100(1):35–46. <https://doi.org/10.2138/am-2015-4856>
- Frantz G (1998) Raman spectra of potassium carbonate and bicarbonate aqueous fluids at elevated temperatures and pressures: comparison with theoretical simulations. *Chem Geol* 152:211–225
- Frost DJ, McCammon CA (2008) The redox state of the Earth's mantle. *Annu Rev Earth Planet Sci* 36:389–420
- Gaetani GA, Grove TL (1998) The influence of water on melting of mantle peridotite. *Contrib Mineral Petrol* 131(4):323–346
- Guillot B, Sator N (2012) Noble gases in high-pressure silicate liquids: a computer simulation study. *Geochim Cosmochim Acta* 80:51–69. <https://doi.org/10.1016/j.gca.2011.11.040>
- Horita J (1988) Hydrogen isotope analyses of natural waters using an H₂-water equilibration method: a special implication to brines. *Chem Geol* 72:89–94
- Horita J, Cole DR, Wesolowski DJ (1995) The activity-composition relationship of oxygen and hydrogen isotopes in aqueous salt solutions; III, vapor-liquid water equilibration of NaCl solutions to 350°C. *Geochim Cosmochim Acta* 59:1139–1151
- Horita J, dos Santos AM, Tulk CA, Chakaoumakos BC, Polyakov VB (2010) High-pressure neutron diffraction study on H–D isotope effects in brucite. *Phys Chem Miner* 37:741–749
- Hunt JD, Kavner A, Schauble EA, Snyder D, Manning CE (2011) Polymerization of aqueous silica in H₂O-K₂O solutions at 25–200 degrees C and 1 bar to 20 kbar. *Chem Geol* 283(3–4):161–170. <https://doi.org/10.1016/j.chemgeo.2010.12.022>
- Javoy M (2004) The early earth evolution. *Geochim Cosmochim Acta* 68:A749–A749
- Kadik A, Pineau F, Litvin Y, Jendrzewski N, Martinez I, Javoy M (2004) Formation of carbon and hydrogen species in magmas at low oxygen fugacity. *J Petrol* 45(7):1297–1310. <https://doi.org/10.1093/ptrology/egh007>
- Kadik AA, Koltashev VV, Kryukova EB, Plotnichenko VG, Tsekhonya TI, Kononkova NN (2014) Solution behavior of C–O–H volatiles in FeO–Na₂O–Al₂O₃–SiO₂ melts in equilibrium with liquid iron alloy and graphite at 4 GPa and 1550 degrees C. *Geochim Int* 52(9):707–725. <https://doi.org/10.1134/s0016702914090067>
- Kennedy GC, Wasserburg GJ, Heard HC, Newton RC (1962) The upper three-phase region in the system SiO₂-H₂O. *Amer J Sci* 260:501–521
- King PL, Holloway JR (2002) CO₂ solubility and speciation in intermediate (andesitic) melts: the role of H₂O and composition. *Geochim Cosmochim Acta* 66(9):1627–1640. [https://doi.org/10.1016/s0016-7037\(01\)00872-9](https://doi.org/10.1016/s0016-7037(01)00872-9)
- Kingsley RH, Schilling J-G, Dixon JE, Swart P, Poreda R, Simons K (2002) D/H ratios in basalt glasses from the Salas y Gomez mantle plume interacting with the East Pacific Rise: water from old D-rich recycled crust or primordial water from the lower mantle? *Geochim Geophys Geosyst* 3:1–26. <https://doi.org/10.1029/2001GC000199>
- Kohn SC, Schofield PF (1994) The importance of melt composition in controlling trace-element behaviour: an experimental study of Mn and Zn partitioning between forsterite and silicate melt. *Chem Geol* 117:73–87
- Kuroda Y, Kariya Y, Suzukoki T, Matsuo S (1982) D/H fractionation between water and the melts of quartz, K-feldspar, albite and anorthite at high temperature and pressure. *Geochem J* 16:73–78
- Kushiro I (1974) The system forsterite-anorthite-albite-silica-H₂O at 15 kbar and the genesis of andesitic magmas in the upper mantle, in geophysical laboratory; igneous petrology, experimental and field studies; volatiles in ultrabasic and derivative rock systems. Carnegie Institution of Washington, Washington, DC, pp 244–248
- Kushiro I (1998) Compositions of partial melts formed in mantle peridotites at high pressures and their relation to those of primitive MORB. In: Fujii T, Dingwell DB, Mysen BO (eds) *Magmatology; the role of magmas in the evolution of the earth*. Elsevier, Amsterdam, pp 103–110
- Le Losq C, Mysen BO, Cody GD (2015) Water and magmas: insights about the water solution mechanisms in alkali silicate melts from infrared, Raman, and ²⁹Si solid-state NMR spectroscopies. *Progr Earth Planet Sci* 2:22. <https://doi.org/10.1186/s40645-015-0052-7>
- Le Losq C, Mysen BO, Cody GD (2016) Intramolecular fractionation of hydrogen isotopes in silicate quenched melts. *Geochem Perspect Lett* 2:87–94
- Luth RW, Boettcher AL (1986) Hydrogen and the melting of silicates. *Am Mineral* 71:264–276
- Luth RW, Mysen BO, Virgo D (1987) Hydrogen in silicate liquids: solution mechanisms of hydrogen in liquids in the system Na₂O - Al₂O₃ - SiO₂ - H₂. *Am Mineral* 72:481–487
- Manning CE (2004) Polymeric silicate complexing in aqueous fluids at high pressure and temperature, and its implications for water-rock interaction. In: Wany RB, Seal RR II (eds) *Water-rock interaction*. Balkema, New York, pp 45–49
- Manning CE, Antignano A, Lin HA (2010) Premelting polymerization of crustal and mantle fluids, as indicated by the solubility of albite plus paragonite plus quartz in H₂O at 1 GPa and 350–620 degrees C. *Earth Planet Sci Lett* 292(3–4):325–336. <https://doi.org/10.1016/j.epsl.2010.01.044>
- Manning CE, Aranovich LY (2014) Brines at high pressure and temperature: thermodynamic, petrologic and geochemical effects. *Precambrian Res* 253:6–16. <https://doi.org/10.1016/j.precamres.2014.06.025>
- Mattey DP (1991) Carbon dioxide solubility and carbon isotope fractionation in basaltic melt. *Geochim Cosmochim Acta* 55(11):3467–3473. [https://doi.org/10.1016/0016-7037\(91\)90508-3](https://doi.org/10.1016/0016-7037(91)90508-3)
- Mattey DP, Taylor WR, Green DH, Pillinger CT (1990) Carbon isotopic fractionation between CO₂ vapour, silicate and carbonate melts: an experimental study to 30 kbar. *Contrib Mineral Petrol* 104:492–505
- McKay NP, Dettman DL, Downs DL, Overpeck JT (2013) The potential of Raman-spectroscopy-based carbonate mass spectrometry. *J Raman Spectrosc* 44:469–474
- Mibe K, Bassett WA (2008) In situ Raman spectroscopic investigation of the structure of subduction-zone fluids. *J Geophys Res* 113. <https://doi.org/10.1029/2007JB005179>
- Morizet Y, Florian P, Paris M, Gaillard F (2017) 17O NMR evidence of free ionic clusters Mⁿ⁺CO₃²⁻ in silicate glasses: precursors for carbonate-silicate liquids immiscibility. *Am Mineral* 102:1561–1564
- Morizet Y, Paris M, Gaillard F, Scaillet B (2010) C–O–H fluid solubility in haplobasalt under reducing conditions: an experimental study. *Chem Geol* 279(1–2):1–16. <https://doi.org/10.1016/j.chemgeo.2010.09.011>
- Mysen BO (2007) Partitioning of calcium, magnesium, and transition metals between olivine and melt governed by the structure of the silicate melt at ambient pressure. *Am Mineral* 92:844–862
- Mysen BO (2009) Solution mechanisms of silicate in aqueous fluid and H₂O in coexisting silicate melts determined in-situ at high pressure and high temperature. *Geochim Cosmochim Acta* 73(19):5748–5763. <https://doi.org/10.1016/j.gca.2009.06.023>
- Mysen BO (2010) Structure of H₂O-saturated peralkaline aluminosilicate melt and coexisting aluminosilicate-saturated aqueous fluid determined in-situ to 800 C and 800 MPa. *Geochim Cosmochim Acta* 74(14):4123–4139. <https://doi.org/10.1016/j.gca.2010.04.024>
- Mysen BO (2012) High-pressure/–temperature titanium solution mechanisms in silicate-saturated aqueous fluids and hydrous silicate melts. *Am Mineral* 97:1241–1251
- Mysen BO (2013) Effects of fluid and melt density and structure on high pressure and temperature experimental studies of hydrogen isotope partitioning between coexisting melt and aqueous fluid. *Am Mineral* 98:1754–1764
- Mysen BO (2015a) Hydrogen isotope fractionation and redox-controlled solution mechanisms in silicate-COH melt plus fluid systems. *J Geophys Res-Solid Earth* 120(11):7440–7459. <https://doi.org/10.1002/2015jb011954>
- Mysen BO (2015b) Carbon speciation in silicate-C–O–H melt and fluid as a function of redox conditions: an experimental study, in situ to 1.7 GPa and 900 degrees C. *Am Mineral* 100(4):872–882. <https://doi.org/10.2138/am-2015-4976>
- Mysen BO (2016) Experimentally-determined carbon isotope fractionation in and between methane-bearing melt and fluid to upper mantle temperatures and pressures. *Earth Planet Sci Lett* 445:28–35
- Mysen BO (2017) Experimental, in-situ carbon solution mechanisms and isotope fractionation in and between (C–O–H)-saturated silicate melt and silicate-saturated (C–O–H) fluid to upper mantle temperatures and pressures. *Earth Planet Sci Lett* 459:352–361

- Mysen BO, Armstrong L (2002) Solubility behavior of alkali aluminosilicate components in aqueous fluids and silicate melts at high pressure and temperature. *Geochim Cosmochim Acta* 66:2287–2298
- Mysen BO, Fogel ML (2010) Nitrogen and hydrogen isotopic compositions and solubility in silicate melts in equilibrium with reduced (N+H)-bearing fluids at high pressure and temperature: effects of melt structure. *Am Mineral* 95:987–999
- Mysen BO, Fogel ML, Cody GD, Morrill PL (2009) Solution behavior of reduced C-O-H volatiles in silicate melts at high pressure and temperature. *Geochim Cosmochim Acta* 73:1696–1710
- Mysen BO, Kumamoto K, Cody GD, Fogel ML (2011) Solubility and solution mechanisms of C-O-H volatiles in silicate melt with variable redox conditions and melt composition at upper mantle temperatures and pressures. *Geochim Cosmochim Acta* 75(20):6183–6199. <https://doi.org/10.1016/j.gca.2011.07.035>
- Mysen BO, Mibe K, Chou IM, Bassett WA (2013) Structure and equilibria among silicate species in aqueous fluids in the upper mantle: experimental $\text{SiO}_2\text{-H}_2\text{O}$ and $\text{MgO-SiO}_2\text{-H}_2\text{O}$ data recorded in situ to 900 degrees C and 5.4GPa. *J Geophys Res-Solid Earth* 118(12):6076–6085. <https://doi.org/10.1002/2013jb010537>
- Mysen BO, Yamashita S (2010) Speciation of reduced C-O-H volatiles in coexisting fluids and silicate melts determined in-situ to ~1.4 GPa and 800°C. *Geochim. Cosmochim. Geochim Cosmochim Acta* 74:4577–4588
- Newton RC, Manning CE (2008) Thermodynamics of $\text{SiO}_2\text{-H}_2\text{O}$ fluid near the upper critical end point from quartz solubility measurements at 10 kbar. *Earth Planet Sci Lett* 274(1–2):241–249. <https://doi.org/10.1016/j.epsl.2008.07.028>
- O'Neil JR, Truesdell AE (1993) Oxygen isotope fractionation studies of solute water interactions. In: Taylor HP, O'Neil JR, Kaplan IR (eds) *Stable isotope geochemistry: a tribute to Samuel Epstein*. The Geochemical Society, Calgary, pp 17–25
- O'Neil JR, Vennemann TW, McKenzie WF (2004) Effect of speciation on equilibrium fractionations and rates of oxygen isotope exchange between $(\text{PO}_4)\text{aq}$ and H_2O . *Geochim Cosmochim Acta* 67:3135–3144
- O'Neill HSC (1991) The origin of the Moon and the early history of the Earth - a chemical model. Part 2: The Earth. *Geochim Cosmochim Acta* 55:1159–1172
- Paillet O, Elphick EC, Brown WL (1992) The solubility behavior of H_2O in $\text{NaAlSi}_3\text{O}_8$ melts: a re-examination of $\text{Ab-H}_2\text{O}$ phase relationships and critical behavior at high pressure. *Contrib Mineral Petrol* 112:490–500
- Papale P, Moretti R, Barbato D (2006) The compositional dependence of the saturation surface of $\text{H}_2\text{O} + \text{CO}_2$ fluids in silicate melts. *Chem Geol* 229:78–95. <https://doi.org/10.1016/j.chemgeo.2006.01.013>
- Pascal ML, Anderson GM (1989) Speciation of Al, Si, and K in supercritical solutions: experimental study and interpretation. *Geochim Cosmochim Acta* 53:1843–1856
- Poulson SR (1996) Equilibrium mineral-fluid stable isotope fractionation factors in graphitic metapelites. *Chem Geol* 131:207–217
- Richter K, Drake MJ (1999) Effect of water on metal-silicate partitioning of siderophile elements: a high pressure and temperature terrestrial magma ocean and core formation. *Earth Planet Sci Lett* 171:383–399
- Rohrbach A, Ballhaus C, Ulmer P, Golla-Schindler U, Schonbohm D (2011) Experimental evidence for a reduced metal-saturated upper mantle. *J Petrol* 52:717–731. <https://doi.org/10.1093/petrology/egq101>
- Saxena SK, Fei Y (1988) Fluid mixtures in the C-H-O system at high pressure and temperature. *Geochim Cosmochim Acta* 52:505–512
- Schiferl D, Nicol M, Zaug JM, Sharma SK, Cooney TF, Wang S-Y, Anthony TR, Fleischer JF (1997) The diamond $^{13}\text{C}/^{12}\text{C}$ isotope Raman pressure sensor system for high temperature/pressure diamond-anvil cells with reactive samples. *J Appl Phys* 82:3256–3265
- Scholze F (1960) Über die quantitative IR-Spektroskopische Wasser-Bestimmung in Silikaten. *Fortschr Mineral* 38:122–123
- Song S, Li S, Niu Y, Zhang L (2009) CH_4 inclusions in orogenic harzburgite; evidence for reduced slab fluids and implication for redox melting in mantle wedge. *Geochim Cosmochim Acta* 73:1737–1754
- Stolper EM (1982) The speciation of water in silicate melts. *Geochim Cosmochim Acta* 46(12):2609–2620
- Taylor WR, Green DH (1987) The petrogenetic role of methane: Effect on liquidus phase relations and the solubility mechanisms of reduced C-H volatiles. In: Mysen BO (ed) *Magmatic Processes: Physicochemical Principles*, pp 121–138
- Ulmer P, Luth RW (1991) The graphite-COH fluid equilibrium in P, T, f_{O_2} space: An experimental determination to 30 kbar and 1600°C. *Contrib Mineral Petrol* 106:265–272
- Van Soest MC, Hilton DR, Kreulen R (1998) Tracing crustal and slab contributions to arc magmatism in the Lesser Antilles Arc using helium and carbon relationships in hydrothermal fluids. *Geochim Cosmochim Acta* 62:3323–3335
- Wang YB, Cody GD, Cody SX, Foustoukos DI, Mysen BO (2015) Very large Intramolecular D-H partitioning in hydrated silicate melts synthesized at upper mantle pressures and temperatures. *Am Mineral* 100:1182–1189
- Wood BJ, Bryndzia LT, Johnson KE (1990) Mantle oxidation state and its relationship to tectonic environment and fluid speciation. *Science* 248(4953): 337–345
- Xue X, Kanzaki M (2008) Structure of hydrous aluminosilicate glasses along the diopside-anorthite join: a comprehensive one- and two-dimensional H-1 and Al-27 NMR study. *Geochim Cosmochim Acta* 72(9):2331–2348. <https://doi.org/10.1016/j.gca.2008.01.022>
- Zhang C, Duan Z, Li M (2010) Interstitial voids in silica melts and implication for argon solubility under high pressures. *Geochim Cosmochim Acta* 74:4140–4149. <https://doi.org/10.1016/j.gca.2010.04.017>
- Zhang Y-G, Frantz JD (2000) Enstatite-forsterite-water equilibria at elevated temperatures and pressures. *Am Mineral* 85:918–925
- Zotov N, Keppler H (2002) Silica speciation in aqueous fluids at high pressures and high temperatures. *Chem Geol* 184:71–82

Submit your manuscript to a SpringerOpen® journal and benefit from:

- Convenient online submission
- Rigorous peer review
- Open access: articles freely available online
- High visibility within the field
- Retaining the copyright to your article

Submit your next manuscript at ► [springeropen.com](https://www.springeropen.com)
